Emergent collectivity in nuclei and enhanced proton-neutron interactions

D. Bonatsos,[1] S. Karampagia,[1] R. B. Cakirli,[2,3] R. F. Casten,[4] K. Blaum,[3] and L. Amon Susam[2]

[1]*Institute of Nuclear and Particle Physics, National Centre for Scientific Research Demokritos, GR-153 10 Aghia Paraskevi, Attiki, Greece*
[2]*Department of Physics, University of Istanbul, Istanbul, Turkey*
[3]*Max-Planck-Institut für Kernphysik, Saupfercheckweg 1, D-69117 Heidelberg, Germany*
[4]*Wright Nuclear Structure Laboratory, Yale University, New Haven, Connecticut 06520, USA*

Enhanced proton-neutron interactions occur in heavy nuclei along a trajectory of approximately equal numbers of valence protons and neutrons. This is also closely aligned with the trajectory of the saturation of quadrupole deformation. The origin of these enhanced *p-n* interactions is discussed in terms of spatial overlaps of proton and neutron wave functions that are orbit-dependent. It is suggested for the first time that nuclear collectivity is driven by synchronized filling of protons and neutrons with orbitals having parallel spins, identical orbital and total angular momenta projections, belonging to adjacent major shells and differing by one quantum of excitation along the *z* axis. These results may lead to a new approach to symmetry-based theoretical calculations for heavy nuclei.

I. INTRODUCTION

In many areas of science, coherence and correlations emerge in complex many-body systems from microscopic ingredients and their interactions. Examples abound in the vibrational, rotational, and bending modes of atoms and molecules and in spatial patterns in complex molecules [1], in collectivity and phase transitions in atomic nuclei, and in similarities to correlations in cold atoms [2]. Similar physics appears in pattern formation in biological entities (e.g., Turing model [3]), cooperativity in biochemical signaling [4], in self-organized social behavior in animal species, in ecological environments [5,6], and in climatic tipping points [7]. The overarching question cutting across disciplines is how assemblages of interacting constituents can develop emerging collectivity not apparent in the individual constituents.

Atomic nuclei provide a fascinating venue for such studies. Their structure is primarily determined by two forces (strong and Coulomb) whose relative strengths are proton number dependent. Further, one can often control the number of interacting bodies (nucleons) and study the particle-number dependence of collective phenomena. Studying how the often simple behavior of nuclei can emerge from nucleonic interactions has been described as one of the great challenges in the study of nuclei [8,9]. The key residual interactions are those among the valence nucleons, and, in particular, the residual valence proton-neutron (*p-n*) interactions [10–14].

It is the purpose of this paper to, first, show newly discovered singular aspects of *p-n* interactions in nuclei with equal or nearly equal numbers of *valence* protons and neutrons and, second, to relate these enhanced interactions to the onset of collectivity. We will then exploit an empirical relation between the single particle quantum numbers of the last-filled proton and neutron orbitals in these nuclei to suggest a simple interpretation of those *p-n* interactions in terms of spatial overlaps of their wave functions. Finally, we show that the nearly synchronous filling of such pairs of orbitals correlates well with the growth and saturation of collectivity. This leads

to a suggestion for a possible new coupling scheme that could greatly simplify symmetry-based shell model calculations.

II. EMPIRICAL *p-n* INTERACTIONS

A measure of the average *p-n* interaction of the last nucleons can be extracted from a double difference of binding energies, called δV_{pn} [15]. In Refs. [16–22] δV_{pn} was related to shell effects and the onset of deformation. In Ref. [23] it was shown that δV_{pn} has large singularities for light $Z = N$ nuclei linked [16] to maximal spatial-spin overlaps of proton and neutron wave functions.

One expects such a phenomenon to dissipate in heavier nuclei where spin-orbit and Coulomb forces grow in importance. And, of course, $Z = N$ nuclei do not exist beyond $A \sim 100$. Thus it came as a surprise that δV_{pn} values in heavy nuclei show similar, though highly muted, peaks [24], as shown in Fig. 1(a), when the number of *valence* neutrons equals the number of *valence* protons or, late in the shells, slightly exceeds the valence proton number. Interestingly, there is a special quantal relation between the last-filled proton and neutron Nilsson [25] orbitals (these are all deformed nuclei) in many nuclei exhibiting these singular δV_{pn} values, namely, that these orbitals are often related by $\Delta K[\Delta N, \Delta n_z, \Delta \Lambda] = 0[110]$, where K and Λ are the projections of the total and orbital angular momenta on the z-axis ($K = \Lambda \pm 1/2$), respectively. If both the oscillator quantum number N ($N = n_x + n_y + n_z$) and the number of quanta in the z direction (the deformation axis), n_z, increase by 1, then $n_x + n_y$ is constant: the two wave functions differ by a single quantum in the z direction and are therefore highly overlapping.

These results concern nuclei with even numbers of protons and the peaks in δV_{pn} were for even-even nuclei. It is well known in such nuclei that the ground state wave functions are spread out over several orbits due to the pairing force. Therefore a much more direct and *pure* perspective is given by odd-odd nuclei where the last protons and last neutrons occupy specific single orbits. Figure 1(b) shows for the first time the
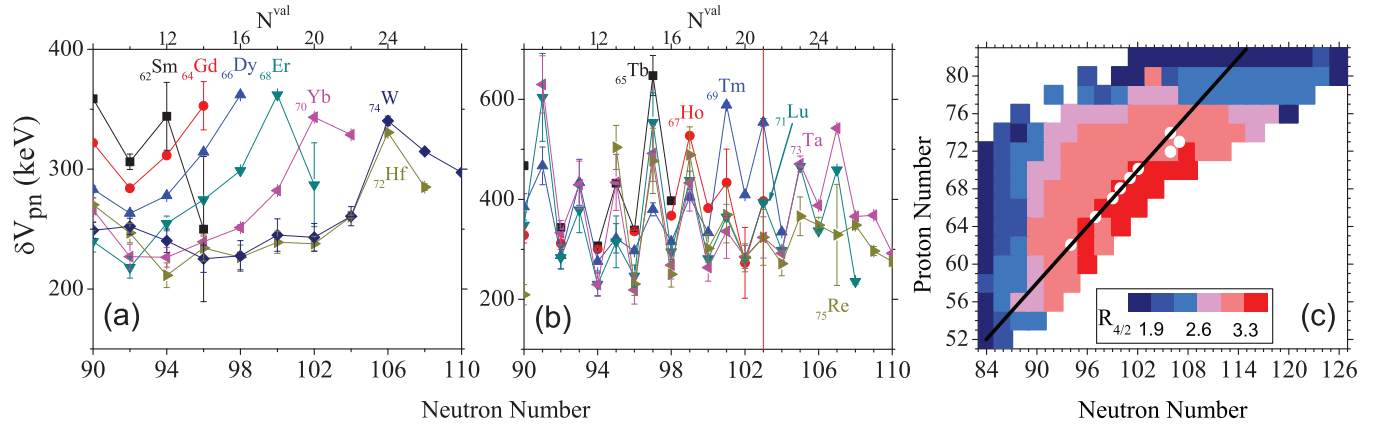
FIG. 1. (Color online) (a) Empirical δV_{pn} values for even-Z nuclei (based on Ref. [24]). (b) Empirical δV_{pn} values for odd-Z nuclei. (c) Color coded contour plot of empirical $R_{4/2}$ values in the $Z = 50$–82, $N = 82$–126 shells. The line drawn represents the line of $Z_{val} = N_{val}$. The white circles are the nuclides for each Z where the largest δV_{pn} value is observed.

empirical results for δV_{pn} for odd-Z nuclei with both even and odd-N. Not only do these results also show spikes, at $Z_{val} \simeq N_{val}$, but now the peaks are sharper and greatly enhanced in magnitude (about four times larger than for even-even nuclei). Figure 1(c) shows the locus of maximum δV_{pn} values in an Z-N plot of $R_{4/2} \equiv E(4_1^+)/E(2_1^+)$, which varies from <2 near closed shells to ~3.33 for well-deformed axial rotors. The results for even-even and odd-odd nuclei closely match both the $Z_{val} \simeq N_{val}$ line and the onset of deformation occurring for $R_{4/2} > 3.3$. This highlights the link to the evolution and saturation of collectivity.

III. A SIMPLE MODEL FOR THE *p-n* INTERACTIONS: CALCULATIONS AND COMPARISON WITH EMPIRICAL RESULTS

How can one try to understand the origin and implications for these results? One approach is large-scale computationally intensive methods such as density functional theory calculations which, indeed, were compared to empirical trends of δV_{pn} in Ref. [20]. While this approach yields good agreement with the data it does not reveal *per se* the underlying origin of the behavior of δV_{pn}. Here we take a much simpler theoretical perspective by directly calculating spatial overlaps of proton and neutron Nilsson wave functions. Our approach in fact obtains similar results but now in a way that explicitly exposes, in a physically intuitive way, the underlying origins of the emergent collectivity through the roles of specific orbitals in *p-n* interactions. As will be seen, this uncovers a heretofore unrecognized pattern in the synchronous filling of proton and neutron orbitals that helps explain the evolution of collectivity and its locus in Z and N.

Nilsson wave functions in the form [25] $\chi_{N\Omega} = \sum_{l\Lambda} a_{l\Lambda}^{\Omega} |Nl\Lambda\Sigma\rangle$ were used, where Ω, Λ, Σ are the projections of the total particle angular momentum j, the orbital angular momentum l, and the spin s on the z axis, while the coefficients $a_{l\Lambda}^{\Omega}$ were calculated by solving the Nilsson Hamiltonian with the standard parameter values, $\kappa = 0.0637$ and $\mu = 0.42$ for neutrons and 0.0637 and 0.6 for protons, respectively. For

axially symmetric nuclei, which we deal with here, K, the projection of the total angular momentum on the z axis, and Ω are the same. Overlaps $\int (\chi_{N_1\Omega_1}^* \chi_{N_1\Omega_1})(\chi_{N_2\Omega_2}^* \chi_{N_2\Omega_2})dV$ were calculated using spherical coordinates. Though the deformation dependence is weak, we used three values, $\epsilon = 0.05, 0.22,$ and 0.3, allocating nuclei to these categories according to $R_{4/2}$ [see Fig. 1(right)], and extending these choices to unknown nuclei using the P-factor [26].

It is instructive to look globally at the overlaps. Figure 2 shows their behavior against correlated differences in K and n_z as well as against differences in each of the Nilsson quantum numbers. In Fig. 2(a) the overlaps are highest when ΔK and Δn_z are small, including the 1[000] case involving proton unique parity orbitals and the case of present interest 0[110]. The overlaps generally fall off for larger ΔK and Δn_z values.

However, one notes two outlying pink boxes at the upper left in Fig. 2(a). These occur for large values of ΔK (3 and even 6) such as the orbital pair 1/2[431] and 13/2[606] and were at first rather puzzling. To understand these and the other patterns we show a further analysis of the overlaps in Figs. 2(b) to 2(f). Each point is an average over all the overlaps for that value of the difference in the relevant Nilsson quantum number. In each case, the overlaps fall off steeply as the particular quantum number differs by larger and larger amounts in the two orbits, peaking at a quantum number difference of zero or one (for ΔN and $\Delta\Lambda$ — see below). Note that the steepest dependence is for the Δn_ρ plot at bottom left, where Δn_ρ is the difference in the number of radial nodes with $n_\rho = (N - n_z - \Lambda)/2$. Finally, the peak at $\Delta N = +1$ is interesting. Given that the maximum overlaps occur for Δn_z and $\Delta n_\rho = 0$, the peak at $\Delta N = +1$ implies a corresponding peak at $\Delta\Lambda = 1$ which is indeed seen. We can now understand the pink boxes with large ΔK in Fig. 2(c). They all correspond to cases of $\Delta n_\rho = 0$ for which the large Δn_ρ overlaps compensate for the large ΔK and Δn_z values. However, such orbit pairs form the ground states only in neutron-rich nuclei not currently accessible.

Figure 3 shows empirical values of δV_{pn} [Fig. 2(a)] and our calculated overlaps [Figs. 2(b) and 2(c)]. Overall the agreement is quite good given the simplicity and parameter free nature of
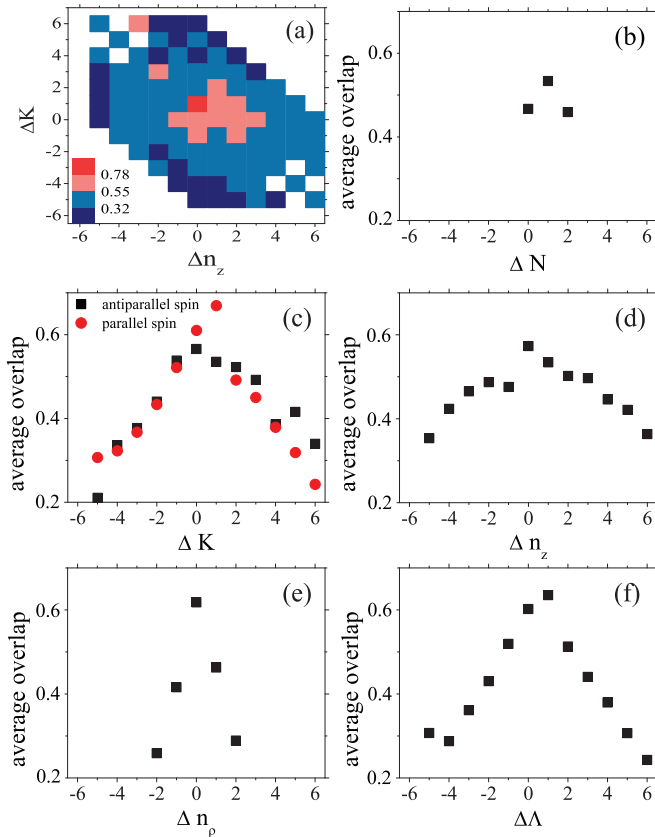
FIG. 2. (Color online) (a) Calculated average spatial overlaps (for a deformation $\epsilon = 0.22$) for proton and neutron orbitals in the $Z = 50$–82, $N = 82$–126 region against the differences (neutron orbit minus proton orbit) in their K and n_z values in a color code. Other panels show average overlaps as a function of differences [(b) ΔN, (c) ΔK, (d) Δn_z, (e) Δn_ρ, and (f) $\Delta \Lambda$] in individual Nilsson quantum numbers.

our approach, and is comparable to that from density functional theory (DFT) calculations [20]. The results generally show small values far from the diagonal, a spread out region of large values early in the shells, and large values near the $Z_{val} = N_{val}$ line that shift slightly to the right of the $Z_{val} = N_{val}$ line towards the end of the shell. A possible reason for this later behavior will be evident below. There are occasional pink boxes to the upper left that disagree with the data. They correspond to very neutron-deficient isotopes for $Z \sim 72$–76. Note also that the blue box for Pb at $N = 124$ would be light pink were zero deformation (instead of 0.05) to be used.

Of course, calculated values are not limited to known nuclei. Figure 3(c) shows overlaps for the full shells. Interestingly, large overlaps now also appear (as in DFT calculations [20]) in neutron-rich nuclei in the region $Z \sim 52$–64 and $N \sim 92$–108. Here pairs of orbitals, such as 5/2[413] with 5/2[512] and 1/2[420] with 1/2[521], coupled to $S = 0$, are filling (near ^{168}Gd and ^{162}Nd, respectively), that do not satisfy 0[110], which implies $S = 1$. Measurement of masses in these regions, which may be available in the future at FAIR, FRIB, and RIKEN, would offer important tests of the current ideas.
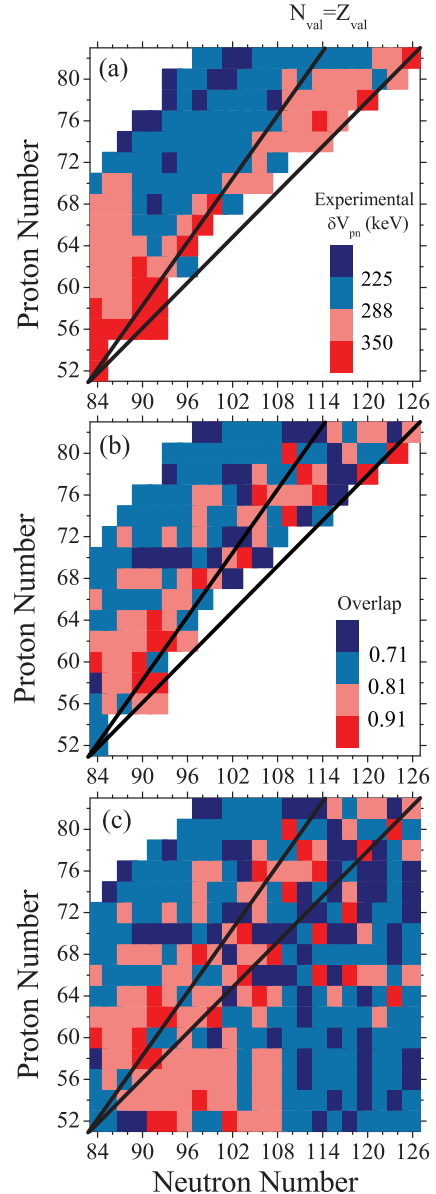

FIG. 3. (Color online) (a) Color coded empirical δV_{pn} values for the $Z = 50$–82 and $N = 82$–126 shells. Large values have redder colors. (b) Similar to (a) but for calculated overlaps for nuclei where empirical values of δV_{pn} are known. (c) Calculated overlaps for the full major shells (excluding nuclei beyond the proton dripline). The upper (lower) black lines represent $Z_{val} = N_{val}$ (equal fractional filling).

IV. IMPLICATIONS FOR THE DEVELOPMENT OF COLLECTIVITY AND DEFORMATION

The idea of *p-n* Nilsson orbital pairs related by 0[110] has a much deeper consequence related to the overall emergence of collectivity in nuclei. In Fig. 4 we show standard proton [Fig. 4(a)] and neutron [Fig. 4(b)] Nilsson diagrams for this mass region. We first note that every one of the 16 Nilsson proton orbitals for the entire shell, including the unique parity orbitals, has a 0[110] neutron partner. This in itself is perhaps not surprising since the neutron shell has one additional
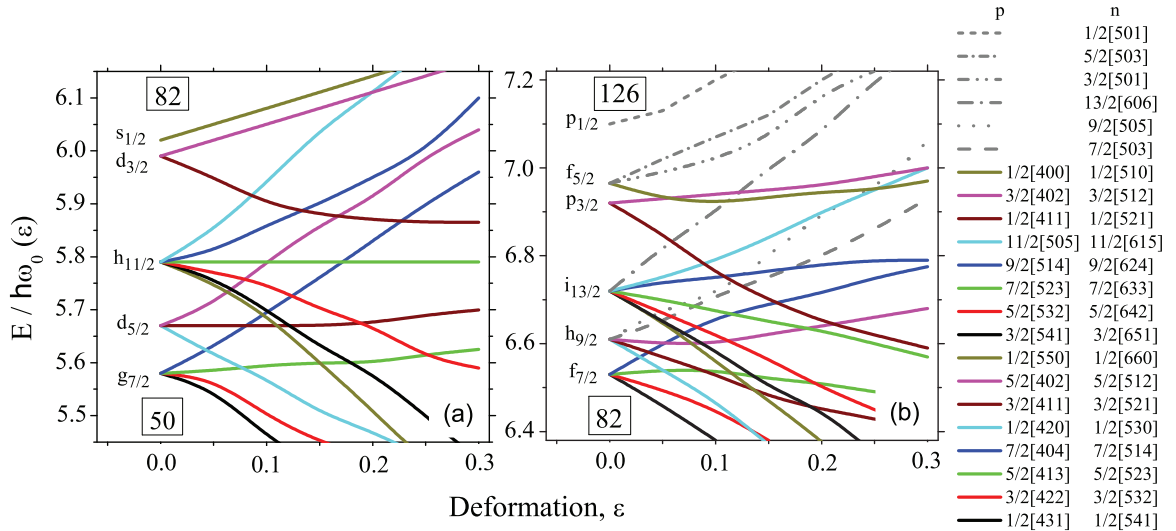
FIG. 4. (Color online) Nilsson diagrams for the proton (a) $Z = 50$–82 and neutron (b) $N = 82$–126 shells. The sequential filling of $\Delta K[\Delta N, \Delta n_z, \Delta \Lambda] = 0[110]$ pairs is closely followed for most deformations in the actual Nilsson diagram as seen by the corresponding color coding of respective proton and neutron orbitals. Neutron orbitals without $0[110]$ proton partners (these have $n_z = 0$) are shown as black lines in the neutron Nilsson diagram.

quantum. However, a closer look shows a general pattern, not heretofore recognized, namely, that, these 0[110] pairs fill almost *synchronously* as the proton and neutron shells fill. This is obvious for small deformations. For example, one has the successive *p-n* combinations: $1/2[431] - 1/2[541]$; $3/2[422] - 3/2[532]$; $5/2[413] - 5/2[523]$; $1/2[420] - 1/2[530]$; and so on. Since the patterns of up- and down-sloping orbits and orbit crossings are similar in the two shells, this synchronous filling of 0[110] combinations approximately persists even as the deformation increases. For example, near midshell for $\epsilon \sim 0.3$, one has, starting at $Z = 68$ and $N = 100$ (18 valence nucleons each): $7/2[523] - 7/2[633]$; $1/2[411] - 1/2[521]$; $5/2[402] - 5/2[512]$; $7/2[404] - 7/2[514]$; $9/2[514] - 9/2[624]$. Except for one interchange of adjacent orbits, these continue to fill in highly overlapping 0[110] combinations even as the deformation changes. This synchronous filling sequence correlates with, and gives a microscopic basis to, the empirical phenomenon of enhanced collectivity along the $Z_{\text{val}} = N_{\text{val}}$ line.

It is only past midshell that neutron orbitals occur (6 of 22) that do not have a 0[110] proton partner. Interestingly, each of these has $n_z = 0$, that is, oblate orbitals that do not contribute to prolate deformation. The interspersing of these rogue $n_z = 0$ orbitals late in the shell interrupts the $Z_{\text{val}} = N_{\text{val}}$ correlation with maximal δV_{pn}, leading to shifts in peaks in δV_{pn} to $N_{\text{val}} = Z_{\text{val}} + 2$ noted earlier (e.g., Hf-W and Lu-Ta region).

V. POSSIBLE NEW PSEUDOSHELL APPROACH TO HEAVY NUCLEI

The 0[110] correlation is repeatedly encountered from the *sd* shell to the actinides. This generality may suggest a new coupling scheme, similar in spirit to the idea of pseudo-SU(3) [27,28], but different in content. The 50–82 major shell is formed by the orbits of the *sdg* oscillator shell, with the

exception that the $1g_{9/2}$ orbit has escaped into the 28–50 major shell, and is replaced by the $1h_{11/2}$ orbit, from the *pfh* oscillator shell. As a result, the $sdg_{7/2}h_{11/2}$ 50–82 shell (with the single orbital 11/2[505] left out) can be considered as an approximate *sdg* shell by replacing the $1h_{11/2}$ orbitals by their 0[110] counterpart $1g_{9/2}$ orbitals. Whereas, in pseudo-SU(3), the entire unique parity orbit is excised, here only the single, highest K, Nilsson orbital is excluded. The new scheme could simplify symmetry-based shell model calculations. Instead of two pseudo-SU(3) shells [with SU(3) subalgebras] plus two shell model single-*j* shells [not possessing SU(3) subalgebras], one has just two approximate shells with SU(3) subalgebras (plus two high-lying high-*K* single orbitals, which can often be ignored), thus deriving from the shell model an approximate SU(3) symmetry for heavy nuclei, at least for $Z_{\text{val}} \simeq N_{\text{val}}$.

As an example, ^{154}Sm is considered, for which the Nilsson deformation parameter is $\epsilon \approx 0.95\beta_2 \approx 0.32$ [25,29]. From Fig. 4 it is clear that 6 of the 12 valence protons occupy normal parity orbitals in the 50–82 shell, while the other six occupy $1h_{11/2}$ orbitals. In addition, six of the ten valence neutrons occupy normal parity orbitals in the 82–126 shell, while the other four occupy $1i_{13/2}$ orbitals.

(i) In the pseudo-SU(3) scheme, the six protons of normal parity sit in the (12,0) irreducible representation (irrep) of U(10) (the pseudoshell formed within the 50–82 shell [27]), while the other six are outside the pseudo-SU(3) symmetry and have to be treated separately. Similarly, the six neutrons of normal parity sit in the (18,0) irrep of U(15) (the pseudoshell formed within the 82–126 shell [27]), while the other four are outside the pseudo-SU(3) symmetry and are treated separately. Thus, one has a (30,0) irrep describing the normal parity nucleons, plus six protons in $1h_{11/2}$ orbitals, plus four neutrons in $1i_{13/2}$ orbitals.

(ii) In the present coupling scheme, using the same group theoretical methods as in Ref. [27], we see that all 12 valence protons sit in the (24,0) irrep of U(15) formed by the 50–82 shell except the high-lying 11/2[505], which plays no role in ^{154}Sm, while all ten neutrons sit in the (30,4) irrep of U(21) formed by the 82–126 shell except the high-lying 13/2[606], which also plays no role. Hence, one has a (54,4) irrep for all valence nucleons in ^{154}Sm.

To proceed further, one has to choose a Hamiltonian containing, in addition to the usual quadrupole-quadrupole and angular momentum terms, SU(3) symmetry preserving third-order and/or fourth-order terms [28,30]. Work in this direction is in progress. Finally, the 0[110] proton-neutron pairs considered in the present work have $S = 1$. The presence of isoscalar $S = 1$ proton-neutron pairs in competition with isovector $S = 0$ nucleon pairs has long been considered in medium mass nuclei with $Z \simeq N$ [31,32]. The present work suggests that similar studies for heavy nuclei with $Z_{val} \simeq N_{val}$.

VI. CONCLUSION

New results, for odd-Z nuclei, show a magnified enhancement of the large empirical values of p-n interactions along the $Z_{val} \simeq N_{val}$ line in a purer form, without the muting effects of pairing. These enhanced values are closely correlated with the development of collectivity, shape changes, and the saturation of deformation. These strong interactions can be simply understood in terms of parameter-free spatial overlaps of special pairs of spin-aligned proton and neutron wave functions differing by single oscillator quanta along the deformation axis. It is precisely these highly interacting 0[110] pairs that fill almost synchronously in heavy nuclei, giving a rationale for the way collectivity develops across major shells. This points to a possible, complementary, new symmetry-based coupling scheme for shell model calculations that is more inclusive than existing schemes.

[1] F. Iachello and S. Oss, Eur. Phys. J. D **19**, 307 (2002).

[2] N. T. Zinner and A. S. Jensen, J. Phys. G **40**, 053101 (2013).

[3] S. Kondo and T. Miura, Science **329**, 1616 (2010).

[4] W. Bialek and S. Setayeshgar, Phys. Rev. Lett. **100**, 258101 (2008).

[5] R. Fossion *et al.*, Symmetries in Nature: Symposium in Memoriam Marcos Moshinsky Aug. 7–14, 2010, Cuernavaca, Mexico, AIP Conf. Proc. **1323**, 74 (2010).

[6] R. Fossion, D. A. Hartasanchez, O. Resendis-Antonio, and A. Frank, Frontiers in Biology **8**, 247 (2013).

[7] T. Lenton, Nature Climate Change **1**, 201 (2011).

[8] NAS-NRC Decadal Report: Nuclear Physics: Exploring the Heart of Matter (Nat. Acad. Sci. 2012).

[9] US DOE/NSF Long Range Plan, The Frontiers of Nuclear Science, DOE/NSF, 2007; NuPECC Long Range Plan 2010: Perspectives of Nuclear Physics in Europe.

[10] A. de Shalit and M. Goldhaber, Phys. Rev. **92**, 1211 (1953).

[11] I. Talmi, Rev. Mod. Phys. **34**, 704 (1962).

[12] P. Federman and S. Pittel, Phys. Lett. B **69**, 385 (1977).

[13] R. F. Casten, D. D. Warner, D. S. Brenner, and R. L. Gill, Phys. Rev. Lett. **47**, 1433 (1981).

[14] T. Otsuka, T. Suzuki, R. Fujimoto, H. Grawe, and Y. Akaishi, Phy. Rev. Lett. **95**, 232502 (2005).

[15] J. D. Garrett and Z.-Y. Zhang, International Conference on Contemporary Topics in Nuclear Structure Physics, Cocoyoc, Mexico, June, 1988; J.-Y. Zhang, R. F. Casten, and D. S. Brenner, Phys. Lett. B **227**, 1 (1989).

[16] P. Van Isacker, D. D. Warner, and D. S. Brenner, Phys. Rev. Lett. **74**, 4607 (1995).

[17] R. B. Cakirli, D. S. Brenner, R. F. Casten, and E. A. Millman, Phys. Rev. Lett. **94**, 092501 (2005).

[18] D. S. Brenner, R. B. Cakirli, and R. F. Casten, Phys. Rev. C **73**, 034315 (2006).

[19] Y. Oktem, R. B. Cakirli, R. F. Casten, R. J. Casperson, and D. S. Brenner, Phy. Rev. C **74**, 027304 (2006).

[20] M. Stoitsov, R. B. Cakirli, R. F. Casten, W. Nazarewicz, and W. Satula, Phys. Rev. Lett. **98**, 132502 (2007).

[21] L. Chen *et al.*, Phys. Rev. Lett. **102**, 122503 (2009).

[22] D. Neidherr *et al.*, Phys. Rev. Lett. **102**, 112501 (2009).

[23] D. S. Brenner, C. Wesselborg, R. F. Casten, D. D. Warner, and J.-Y. Zhang, Phys. Lett. B **243**, 1 (1990).

[24] R. B. Cakirli, K. Blaum, and R. F. Casten, Phys. Rev. C **82**, 061304(R) (2010).

[25] S. G. Nilsson, Mat. Fys. Medd. K. Dan. Vidensk. Selsk. **29**, 16 (1955).

[26] R. F. Casten, D. S. Brenner, and P. E. Haustein, Phys. Rev. Lett. **58**, 658 (1987).

[27] R. D. Ratna Raju, J. P. Draayer, and K. T. Hecht, Nucl. Phys. A **202**, 433 (1973).

[28] J. P. Draayer and K. J. Weeks, Ann. Phys. (NY) **156**, 41 (1984).

[29] S. Raman, C. W. Nestor, Jr., and P. Tikkanen, At. Data Nucl. Data Tables **78**, 1 (2001).

[30] G. Vanden Berghe, H. E. De Meyer, and P. Van Isacker, Phys. Rev. C **32**, 1049 (1985).

[31] P. Federman and S. Pittel, Phys. Rev. C **20**, 820 (1979).

[32] F. Šimkovic, Ch. C. Moustakidis, L. Pacearescu, and A. Faessler, Phys. Rev. C **68**, 054319 (2003).